Supplementary material

Table S1*: The elemental composition of the bulk alloy, x (at.%), and mean free path λ (nm) for each element in the alloy used in the calculation of information depth at 4 keV. The λ values* were *obtained by using the software QUASES-IMFP-TPP2M Ver. 3.0 [1].*

Element	**Fe**	**Cr**	**Ni**	**Mo**	**Mn**	**Si**	**N**	**Cu**	**P**	**C**	**S**	**Tot**
x (at%)	61.6	26.4	6.5	2.2	0.8	1.2	1.1	0.2	<0.1	0.1	<0.1	100
λ (nm)	4.8	5.1	4.6	4.9	5.0	7.3	8.6	4.6	7.6	8.7	7.3	5.0

Calculation of thickness and composition of the oxide and hydroxide layers

In the following equations, the superscripts of 'in', 'out', and 'met' refer to the inner layer, the outer layer, and the metallic components, respectively. The thickness and Cr content of the inner layer was calculated by solving the following dependent equations (eq. (3) in the paper) for Cr and Fe, respectively:

$$d_{in} = \lambda_{\mathbf{Cr}}^{in} \sin(\theta) \cdot \ln\left(1 + \frac{I_{Cr}^{in} \cdot D_{Cr}^{met} \cdot \lambda_{Cr}^{met}}{I_{Cr}^{met} D_{\mathbf{Cr}}^{in} \lambda_{Cr}^{in}}\right) \quad \text{eq. (1)}$$

$$d_{in} = \lambda_{\mathbf{Fe}}^{in} \sin(\theta) \cdot \ln\left(1 + \frac{I_{Fe}^{in} \cdot D_{Fe}^{met} \cdot \lambda_{Fe}^{met}}{I_{Fe}^{met} D_{\mathbf{Fe}}^{in} \lambda_{Fe}^{in}}\right) \quad \text{eq. (2)}$$

where $D_{Cr}^{in} = \frac{\rho_{Cr}^{in}}{M_{Cr}^{in}} \cdot x_{Cr}^{in}$ and $D_{Fe}^{in} = \frac{\rho_{Fe}^{in}}{M_{Fe}^{in}} \cdot x_{Fe}^{in}$. Moreover, $x_{Fe}^{in} = \left(1 - x_{Cr}^{in}\right)$ because the passive film is assumed to consist only of Cr and Fe. Thereby the layer thickness and Cr content can be obtained by solving the two equations with the two unknown parameters, d_{in} and x_{Cr}^{in}.

For the outer layer, the thickness d_{out} and Cr content x_{Cr}^{out} were obtained from in a similar approach as above, using the calculated d_{in} and x_{Cr}^{in} and the following equations (eq (4) in the paper) for Cr and Fe, respectively:

$$d_{out} = \lambda_{Cr}^{out} \sin(\theta) \cdot \ln\left(1 + \frac{I_{Cr}^{out} D_{Cr}^{in} \lambda_{Cr}^{in}}{I_{Cr}^{in} D_{Cr}^{out} \lambda_{Cr}^{out}}\right) \cdot \left(1 - EXP\left(-\frac{d_{in}}{\lambda_{\mathbf{Cr}}^{in} Sin(\theta)}\right)\right) \quad \text{eq. (3)}$$

$$d_{out} = \lambda_{Fe}^{out} \sin(\theta) \cdot \ln\left(1 + \frac{I_{Fe}^{out} D_{Fe}^{in} \lambda_{Fe}^{in}}{I_{Fe}^{in} D_{Fe}^{out} \lambda_{Fe}^{out}}\right) \cdot \left(1 - EXP\left(-\frac{d_{in}}{\lambda_{\mathbf{Fe}}^{in} Sin(\theta)}\right)\right) \quad \text{eq. (4)}$$

where $D_{Cr}^{out} = \frac{\rho_{Cr}^{out}}{M_{Cr}^{out}} \cdot x_{Cr}^{out}$ and $D_{Fe}^{out} = \frac{\rho_{Fe}^{out}}{M_{Fe}^{out}} \cdot (1 - x_{Cr}^{out})$.

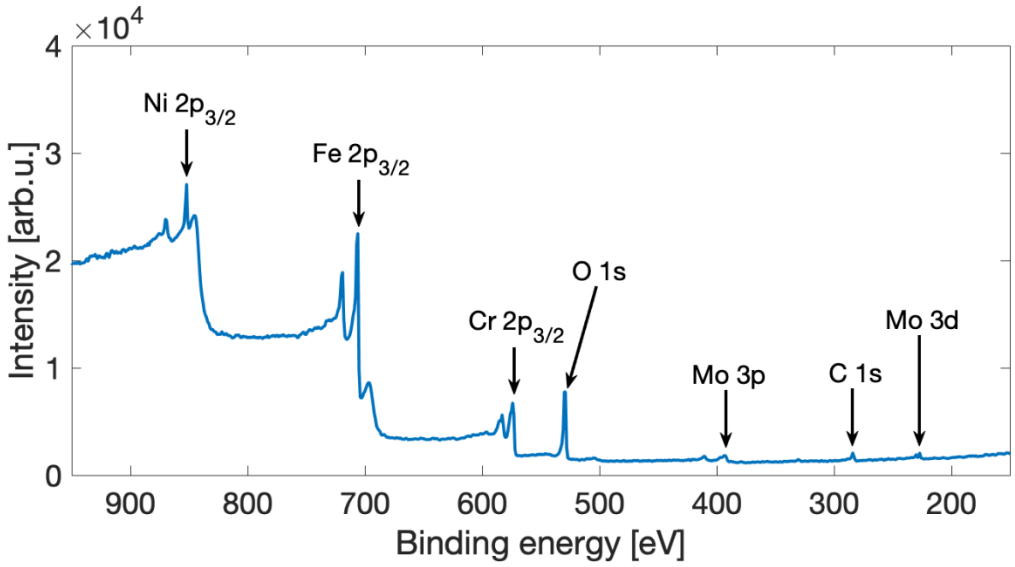

Figure S1: HAXPES survey spectrum of the duplex stainless steel sample, showing strong peaks of Fe, Cr, Ni, O, and weak but detectable signals of Mo. The binding energy of Fe 2p in metallic state in the HAXPES data was used for calibration of the HAXPEEM data after correction of the statically charge using C 1s peak.

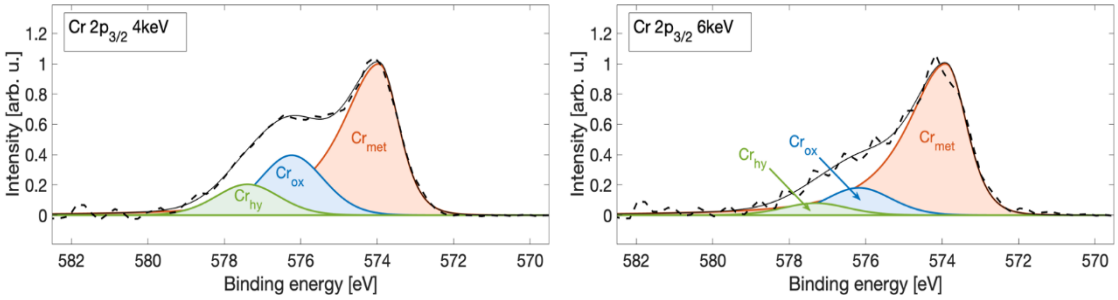

Figure S2: Summed XPS spectra of Cr $2p_{3/2}$, extracted from the HAXPEEM data obtained at 4 keV and 6 keV (less surface sensitive), for the whole measured area including the analyzed and non-analyzed grains. The data show an intensity decrease of 46% for the oxide and 50% for the hydroxide. The larger decrease of the hydroxide peak intensity indicates that hydroxide is mainly present at the outermost layer.

Box plots showing the distribution of data from individual grains

Box plot is a way of showing the distribution of the individual values of the data. In a box plot, the median line marks 50% of the data. If this line of one of the boxes exaggerates the top of another box (the top of the box marks 75% of the box data), it means that 50% of one box data are higher than the compared box and thereby a difference is likely. If the median line exaggerates the other box completely including the whiskers of the other box or boxes, it means that there is a difference between the box plots [2].

The following box plots show the data distribution of the individual grains included in the two phases (Figure S3) for Cr content, in the three orientations for the layer thickness (Figure S4), and Cr content (Figure S5), respectively. A brief explanation of the data in each figure is given under the figure.

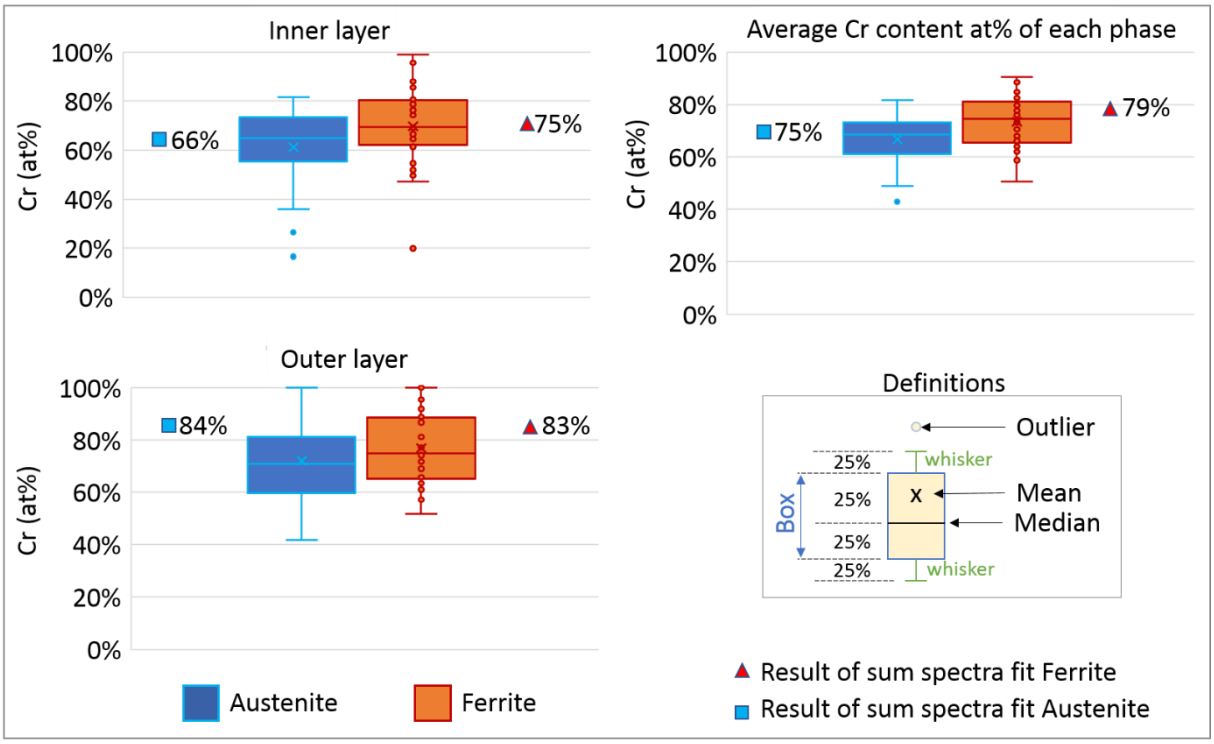

Figure S3. Box plot showing Cr content of the inner layer, outer layer, and average of the whole native passive film.

In this figure, the median line for the average Cr content for ferrite data exaggerates the top of the box for austenite data. This means that there is likely a difference in the average Cr content of the native passive film between the two phases, which is higher on ferrite than on austenite.

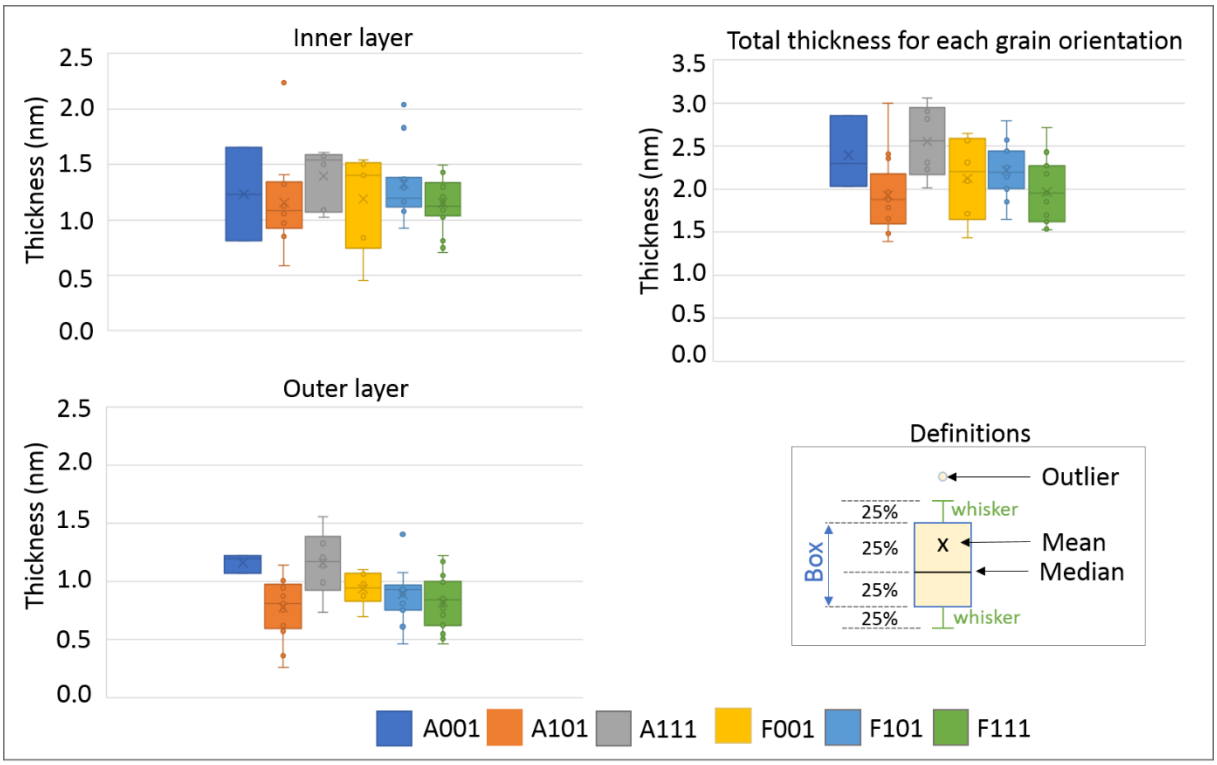

Figure S4. Box plot showing the thickness of the inner layer, outer layer, and whole native passive film for each grain orientation.

In this figure, the box plot shows that the thickness of outer layer is significantly thicker for austinite (001) than austenite (101) as well as ferrite (101) and (111), due to that the median marking 50% of the austenite (001) data exaggerates the full boxplots of the mentioned orientations. It is also likely that austinite (001) and (111) have a larger total thickness compared to the other orientations.

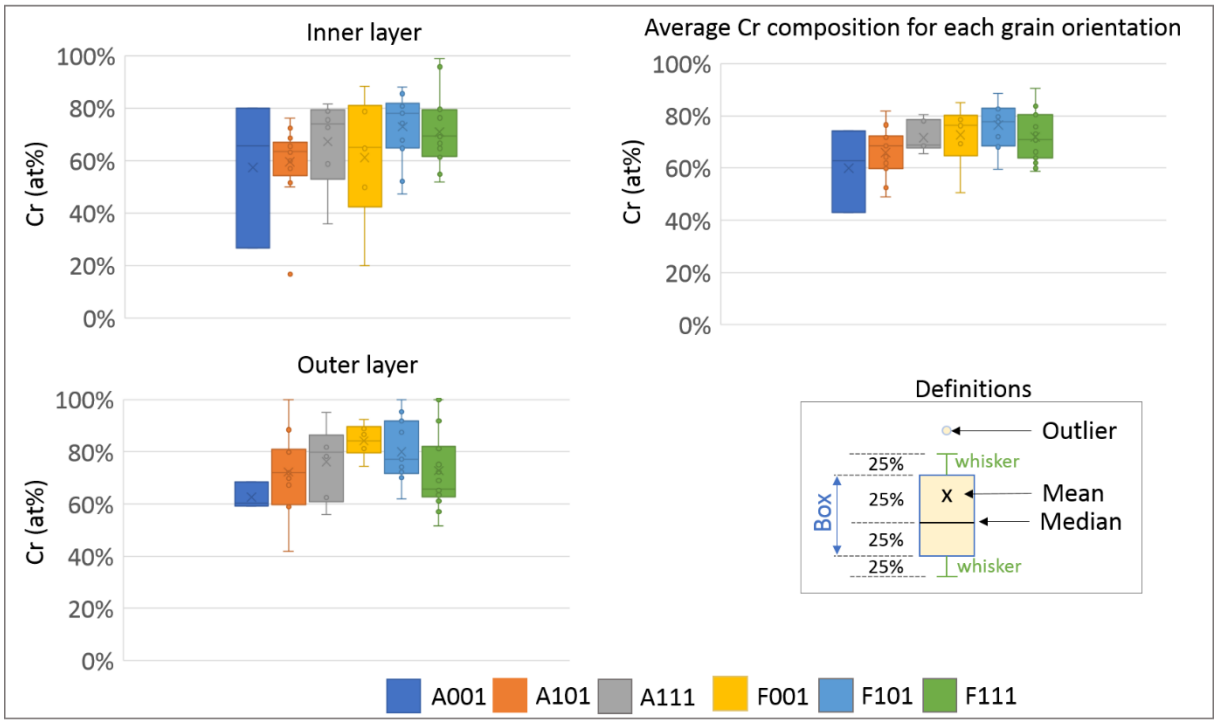

Figure S5. Box plot showing the Cr content (at%) for the inner and outer layer as well as the average for the whole native passive film for each phase and grain orientation.

In this figure, the box plot shows that there is likely difference in the Cr content of the outer layer, i.e., ferrite (111) seems to have lower Cr content compared to the other ferrite grains. There are also likely differences between different orientations, e.g., austenite (111) seems to have a higher Cr content, especially in the outer layer, compared to the other austenite orientations.

References

1.Tougaard, S., *QUASES Software packages to characterize surface nanostructures by analysis of electron spectra* http://www.quases.com/. May 2019.

2.*https://maths.nayland.school.nz/Year_11/AS1.10_Multivar_data/11_Comparing_Boxplots.htm.* April 2020.